REMESHING ALGORITHM FOR MULTIRESOLUTION PRIOR MODEL IN SEGMENTATION

A. Gouaillard[(1) (2)], A. Gelas[(1) (2)], S. Valette[(3)], E. Boix[(1)], T. Kanai [(2)], and R. Prost[(1)]
[(1)] CREATIS, Lyon, France; [(2)] KANAI, Keio University, Tokyo, Japan; [(3)] LIS, Grenoble, France.

ABSTRACT

We consider the construction of a multiresolution triangular mesh for 3D model-based segmentation. In the 3D Snake approach this model needs to be both uniform and regular for convergence purposes. We propose here a remeshing algorithm to compute such a model from an arbitrary triangular mesh. The input mesh is first parameterized in 2D. The output mesh connectivity is fixed by a subdivided base mesh. Its geometry comes from the input mesh via the parametric domain tessellation with respect to uniformity constraints. Experiments were carried out with both synthetic and organ models. They prove the low geometry remeshing error and the uniformity of the resulting mesh.

1. INTRODUCTION

X-ray Computed Tomography (CT), Magnetic Resonance Imaging technique (MRI), Positron Emission Tomography (PET) produce large 3D images. When extracting anatomic features from voxel data using segmentation we are faced with decision uncertainty due to different tissues that produce quite similar gray levels. In most cases the shape of the anatomic feature is approximately known. Such knowledge can be used to construct a geometrical a-priori model of the anatomic feature of interest. The model is then used as an initialization of a Snake algorithm to improve its robustness and the quality of the results.

Some biomedical applications (screening of transgenic mice, for example) require rapid segmenting of the data to reach acquisition rate and analysis automation constraints. For such applications, the model and the volume can be decomposed into several levels of details, each being the approximation of the previous one and used in an iterative, multiresolution segmentation algorithm. This approach both enhances the robustness and reduces significantly the computation cost. It was proved effective in 2D [3]. We have in mind to extend this approach in 3D based on a general 3D multiresolution scheme [13].

The extension of that framework to 3D proved to be delicate. In practice the fine mesh model is extracted from a reference volume using the Marching Cube Algorithm. The resulting mesh contains thousands to millions of triangles and is irregular, i. e. there are many stretched triangles and the connectivity is highly irregular. This results in numerical instabilities during the snake evolution. The usual solution to overcome this problem is to resample the surface during the segmentation when a quality indicator goes below a threshold. Unfortunately, we cannot resample the approximations of the original mesh. The details are computed before the segmentation process. Details are defined as differences between two approximations and depend on their connectivity. Resampling one of the approximations would change its connectivity and thus the details would not be relevant any more. In other words, resampling would break the multiresolution representation of the model.

Supposing that with a good initialization (always possible with a registration at coarse level), the displacements of the nodes of the mesh are small, we need to have a uniform and regular multiresolution model to avoid resampling. To achieve higher processing rates, it is desirable not to resample during the segmentation but before the segmentation. The multiresolution model should be built once only before processing the data. In this paper we propose a novel remeshing algorithm to create such a model.

The novelty of this algorithm can be summarized as follows:

1. It is applied prior to the segmentation (offline).
2. It builds multiresolution meshes.
3. It takes into account the constraints associated with the snake algorithm: uniformity and regularity.

The paper is organized as follows. Section 2 introduces basics about discrete active contours and points out constraints resulting from the discretization of the algorithm. Section 3 gives an overview of the existing remeshing solutions. Section 4 describes our proposed algorithm. Results and discussion conclude this paper.

2. DISCRETE ACTIVE CONTOUR

The reader can refer to [12] for an extensive explanation on deformable surfaces.

A snake, [4,6], is a surface in a volume which dynamically updates its position according to the minimization of an energy functional E. As we are using discrete surfaces, we are going to apply the equation only at a discrete set of locations (vertices). Using finite differences, we can define a discrete approximation of E. This supposes that the surface is uniformly sampled. Snake convergence requires uniformly sampled surfaces.

0-7803-8554-3/04/$20.00 ©2004 IEEE.

Also note that, for discrete contours, expressing the first order and second order derivatives is easy, but that it is not possible for discrete surfaces like triangulations. Only estimators are available which can lead to too coarse or even wrong estimation if the surface connectivity is not regular enough. For the estimation of curvature, we need the model to be as regular as possible.

3. MULTIRESOLUTION AND REMESHING

Remeshing consists in modifying sampling and connectivity of a given mesh to create a new one, with the same geometry. Many remeshing algorithms have been proposed in the literature.

Most of the remeshing algorithms that build multiresolution mesh [5,8,9] start with a base mesh with a low number of vertices which best approximate the geometry of the original mesh. They then subdivide regularly each triangle into four. The resulting mesh is semi-regular: every vertex has valence six except some vertices of the base mesh.

Recently two algorithms to uniformly remesh a given surface have been proposed [1,2]. First a "density function" or "map of interest" is computed in a parametric domain $D \in \Re^2$. Then D is point-sampled with respect to a density function using an error diffusion algorithm (Half-toning). Alliez et al build a Delaunay triangulation out of this point sampling and finally improve the resulting mesh. In [1] this improvement is based on univariate laplacian smoothing, whereas [2] uses Lloyd's algorithm [10,11] to converge to a Centroidal Voronoï Tessellation (CVT).

Since the remeshing algorithms of both [1,2] are based on point sampling and does not take connectivity into account, those techniques can not produce multiresolution meshes.

4. PROPOSED ALGORITHM

4.1 Notation and definitions

Assume a given input mesh $M = (V, E, F)$ where V is the set of vertices $V = \{p_i\}$ in $\Re^3$, E is the set of edges, and F is the set of triangular faces $F = \{t_j\}$. The set V defines the geometry; E and F define the connectivity of the mesh M. A subdivision connectivity mesh S of L levels has the further property of being a refinement of a base mesh S^0, i.e., it is the last element of a sequence of meshes

$$S^0 \ldots S^j, S^{j+1} \ldots S^L .$$

We denote

$$S^j = (V^j, E^j, F^j), \; j \in [0, L],$$

the j-th 1:4 subdivided mesh of the base mesh S^0 where each edge is split into two new edges and each face is split into four new faces.

A parameterization consists in constructing a mapping Λ (an isomorphism), i.e. a piecewise, linear, one-to-one correspondence between each triangle of the original 3-D mesh M, and its image in a 2-D convex domain $D \in \Re^2$. This isomorphism requires a mesh with a boundary. If the input mesh is boundary-free we apply the parameterization on two parts of the mesh [7] or by patches [5,9]. We denote

$$T = \Lambda(M)$$

the parameterization of the input mesh M, and

$$T^0 \ldots T^j, T^{j+1} \ldots T^L$$

that of a subdivision connectivity hierarchy S^j. Note that the connectivity graph of T is identical to that of M.

4.2 Basic ideas behind our proposal

In our approach the connectivity of the new model will be defined by that of a subdivided base mesh. The connectivity will be defined directly in D, using a parameterization of the original surface. This will give us the regularity.

Unfortunately this approach results in a uniform sampling rate in $D \in \Re^2$ but not in $\Re^3$ due to the distortion of the surface caused by the parameterization. The distortion of the triangle area can be computed at parameterization step. For a given triangle and its corresponding triangle in D the distortion is defined as

$$d = \frac{A_{2D}(t_i)}{A_{3D}(t_i)},$$

To enforce uniformity of the created model in $\Re^3$ we solve the following inverse problem: move the vertices of the created model in D in order to compensate for the distortion. A solution has been independently proposed for this inverse problem in [1] and [2] but without consideration of the connectivity problem.

We propose here to combine the subdivision rule and a relaxation method inspired by [2] and presented more in detail in 4.4 to build each resolution of our model. This approach is novel in the sense that it uses relaxation within the process and not as a post process. Thus, each T^j is as uniform as possible, with respect to the sampling rate that is quite low at coarse levels. It doesn't need to reprocess every approximation to improve them, which would be the case if you used a relaxation and then lifting scheme.

4.3 Overview of our algorithm

Our algorithm consists in the following steps:

1. Initialization.
   (a) Build the parameterization Λ of M on D ,
   (b) Compute area distortion for every triangle,
   (c) Construct the base mesh T^0 in D
2. For all resolution levels j, build T^{j+1}
   (a) Subdivide each T^j face 1 to 4
   (b) Move the new vertices in D (see 4.4)
   (c) Compute S^{J+1} from its parameterization T^{j+1} using barycentric coordinates interpolation method as in [7].

4.4 Parametric Domain Tesselation by Lloyd's Algorithm

Following [2], in order to resample the input surface in the parametric domain D with respect to a density function we tessellate D.

The Lloyd's algorithm (LA) [10,11] is a fixed point algorithm that is used to compute Centroïdal Voronoï tessellation (CVT). In [2] it is used on the 2D case of CVT to improve the placement of the vertices. The method showed good behavior, improving the uniformity of the mesh when using the area stretch factor as density function.

Our derivation of this method overcomes the following drawback. For arbitrary 2-manifolds the Voronoï cell can extend outside the 1-ring if it has obtuse triangles. In that case LA moves the vertex anywhere inside the Voronoï cell. If the vertex is moved outside of the 1-ring, triangle flips occurs. (See Fig.1)

We propose here another neighborhood definition N that still defines a tessellation and where triangles are never flipped when applying the Lloyd's algorithm. We compute the barycenter of each triangular cell into the 1-ring of v. and the middle point of each edge using the vertex v. One can check that we defined a tessellation:

- To one vertex v corresponds one and only one N ,
- The union of all N defines D,
- The intersection of two neighborhoods is empty,

We also enforced the desired property of N always lying within the 1-ring of the vertex.

Now we have defined a neighborhood with respect to connectivity we can implement the rest of the algorithm as in [2]. The density function will be chosen as the triangle stretching factor to build an as uniform as possible mesh. For each vertex v the stretching factor is equal to

$$s = \sum_{N} d' ,$$

where d' is a fraction of d with respect to the area of each triangle of the 1-ring covered by N.

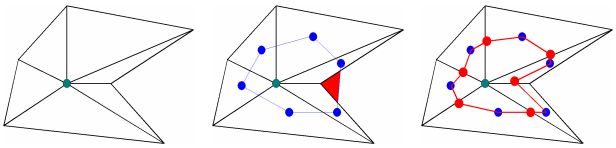

Fig. 1: *Left picture: a vertex with a non-convex 1-ring. If we use the dual cell there is a "flip-zone" (central picture, colored zone). On the right, that with our definition, the neighborhood is constrained within the 1-ring.*

5. RESULTS AND CONCLUSION

We ran our algorithm on three models: synthetic model of aneurysm, dog heart model and mushroom model.

We computed first the geometrical inaccuracy as the mean square distance between the original mesh and the remeshed one. The multiresolution algorithm ran without the relaxation algorithm first to measure the impact of the relaxation scheme.

Fig. 2 is an overview of our result. Note that relaxing using our algorithm enhances the mesh quality: lower geometrical error, bigger minimum angle, lower variance and better shape factor. These good results are constant across the resolutions of the remeshed surface and across the models. Our experiments showed that the quality could be further improved by improving the base mesh and the quality of the parameterization. We are thinking about improving the parameterization by means of conformal energy minimization in the future.

6. ACKNOWLEDGMENTS

This work was supported in part by INRIA ARC Télégéo. The authors would like to thank Pierre Alliez both for his helpful comments and suggestions. The authors thank D. P. Hanson and R. Robb, Mayo Foundation, Rochester, Minnesota USA for providing the DSR Image of the left ventricular of a dog used in this paper.

7. REFERENCES

[1] P. Alliez, M. Meyer, M. Desbrun, "Interactive Geometry Remeshing," *ACM Transactions on Graphics (Proc. SIGGRAPH'02)*, pp. 34~354, 2002.

[2] P. Alliez, E. Colin De Verdiere, O. Devillers, M. Isenburg. "Isotropic Surface Remeshing," *SMI'03*, 2003.

[3] E. Chereul, A. Gouaillard, R. Prost, C. Odet, "Segmentation d'images par deformation multiresolution sur base d'ondelettes combinant modele et donnes," *GRETSI'03*, 2003.

[4] L. D. Cohen, "On active contour models and balloons," *Computer Vision, Graphics and Image Processing: Image Understanding*, 1991, Vol. 53, N° 2, pp. 211-218.

[5] M. Eck, T. DeRose, T. Duchamp, H. Hoppe, M. Lounsbery andW. Stuetzle, “MAPS: Multiresolution Analysis of Arbitrary Meshes”. *ACM computer graphics (Proc. SIGGRAPH'95)*, pp. 173 -182,1995.

[6] M. Kass, A. Witkin, et D. Terzopoulos. "Snakes: active contour models," *International Journal of Computer Vision*, 1988, Vol. 1, N° 4, pp. 321-331.

[7] Y. S. Kim, S. Valette, and R. Prost Adaptive Wavelets Based Multiresolution Modeling of Irregular Meshes Via Harmonic Maps*, ICIP'01*, Thessaloniki, Greece, Vol. 3, pp. 210-213, October 2001

[8] L. Kobbelt, J. Vorsatz, U. Labsik, H.P. Seidel, “A Shrink Wrapping Approach To Remeshing Polygonal Surfaces,” *Computer Graphics Forum (Proc. EUROGRAPHICS '99)*, pp. 119-130, 1999.

[9] A. Lee, W. Sweldens, P. Schrder, L. Coswar, and D. Dobkin, “Multiresolution Adaptive Parameterization Of Surfaces,” *ACM Computer Graphics (Proc. SIGGRAPH'98)*, pp. 95 ~ 104, 1998.

[10] Y. Linde, A. Buzo and M. Gray, “An algorithm for vector quantizer design,” *IEEE Transaction on Communication*, 1980.

[11] S.P. Lloyd, “Least Square Quantization in pcm,” *Technical note, Bell Laboratories, 1957. Published in IEEE Transaction on Information Theory*, Vol. 28, pp. 129-137, 1982.

[12] J. Montagnat and H. Delingette, “A review of deformable surfaces: topology, geometry and deformation,” *Image and Vision Computing*, 19(14):1023-1040, December 2001.

[13] S. Valette, and R. Prost, Wavelet Based Multiresolution Analysis of Irregular Surface Meshes, *IEEE Transactions on Visualization and Computer Graphics,* Vol. 10, No. 2, March/April, pp. 113-122, 2004.

	Source	No-Relax 16k	Relax 16k	Relax 4k	Relax 1k
Aneurysm	13.2 0 0.6 0.18	0.473% 14.798 0,006 1.3 0.40	0,022% 35.4 0.18 1.09 0.41	0,078% 34.3 1.14 2.17 0.43	0,293% 34.3 3.42 4.17 0.44
Heart		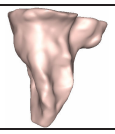			
Heart	14.2 15.8 2.02 0.82	0,481% 22.0 0.004 5.72 0.53	0,021% 23.3 8.1 2.0 0.7	0,044% 23.2 10.5 4.2 0.68	0.154 % 22.5 16.2 8.5 0.68
Mushroom	23.4 8.9 0,02 0.64	27.7 8.04 0.07 0.60	24.2 14.3 0,02 0.65	24.4 14.4 0,05 0,65	24.4 15.36 0,10 0.65

Fig. 2: *Results of our algorithm on three models. From top to bottom, we show results using a synthetic model of an aneurysm, dog heart model and mushroom model of figure 3. For each mesh, the geometrical inaccuracy (as a percentage of the bounding box diagonal), the variance of angles, the minimum angle; the variance of edge length and shape factor are given in that order. Each column gives results depending on the requested number of triangles for the resulting model.*

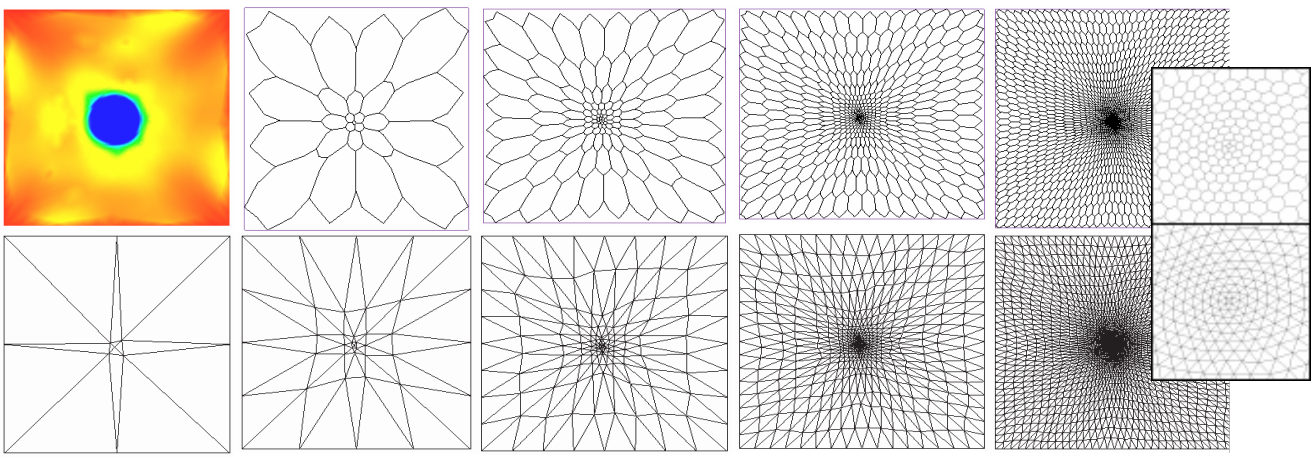

Fig. 3: *top left: D colored with the density function; the first row illustrates the evolution of the neighborhoods at different resolutions; the second row illustrates the evolution of the corresponding mesh on D. The zoom on the right shows the great uniformity of both the neighborhood and mesh after convergence.*